Dual-band Circular Polarizer and Linear Polarization Transformer Based on Twisted Split-Ring Structure Asymmetric Chiral Metamaterial

Yong Zhi Cheng[1], Yie Nie[1, *], Zheng Ze Cheng[2], and Rong Zhou Gong[1]

Abstract—In this paper, a bi-layer twisted split-ring structure asymmetric chiral metamaterial was proposed, which could achieve circularly polarized (giant circular dichroism effect) wave with dual bands and linear polarization transformation (giant optical activity) with asymmetric transmission wave emissions simultaneously from linearly polarized incident wave at microwave frequencies. Experiment and simulation calculations are in good agreement, indicating that the dual-band circular polarizer features high conversion efficiency around 5.32 GHz and 6.6 GHz in addition to large polarization extinction ratio of more than 16 dB, while cross linear polarization transformation with asymmetric transmission is observed around 10.52 GHz. The transformation behavior for both circular and linear polarizations could be further illustrated by simulated surface current and electric field distributions. The proposed asymmetric chiral metamaterial structure could be useful in designing novel EM or optical devices, as well as polarization control devices.

1. INTRODUCTION

Since Tretyakov et al. and Pendry predicted theoretically that a chiral route can be used in order to obtain negative refraction [1, 2], the chirality concept in metamaterials (MMs) has attracted significant attention. Chiral metamaterials (CMMs) is a subset of MMs, which have no symmetric planes and are not identical to their mirror images, and also neither violates reciprocity nor time-reversal symmetry, leading to cross-coupling between the electric and magnetic fields [3]. CMMs are of great current interest both for customized functionalities and for potential applications not found in natural medium arise from the magneto-electric cross coupling of chiral structures due to their lack of any mirror symmetry. As a fact, besides negative refractive index, CMMs can also achieve other exotic EM characteristics, such as giant gyrotropy [4], strong polarization rotation (giant optical activity) [5–11], circular polarizer (circular dichroism, CD effect) [12–15], asymmetric transmission (AT) effect [16–21], linear or/to circular polarization conversion [22–32], and even the prospect of a repulsive Casimir force [33, 34] by special enantiomeric forms or similar chiral structure design. The cross-coupling is original physics of these special electromagnetic (EM) properties [35, 36].

Manipulating polarization state of EM waves or light is critical for a wide range of applications, such as liquid crystal display, wireless communications, optical data storage and so on [36, 37]. Thus, the effective manipulation of EM wave polarization is highly desirable [21]. Compared with conventional media or method [38, 39], CMMs has some advantages to realize the manipulating polarization, such as high polarization conversion efficiency and operation frequency can be scaled to different EM spectrum due to the geometry scalability. Based on this, there have been many efforts tending toward the realization of the CMMs in manipulating the polarization states of EM wave [12–31] with high efficiency.

Recently, a set of circular polarizers (giant CD effect) [12–15, 22–32] and pure linear polarization rotators or transformers with AT effect [16–21] using helix structure, asymmetric U-shaped SRR pair, planar spiral structure, and twisted split ring resonators (SRRs), more concentric rings and other asymmetric chiral structures have been intensively reported. Among them, all these chiral structures could be available to tailor the cross coupling between electric and magnetic fields, which can achieve a giant CD effect or optical activity or circular conversion dichroism. It means that the conversion of different polarization states of EM waves can be realized by these CMMs, such as linear to linear [16–21, 27, 31, 32], linear to circular [22–28, 31, 32], and circular to circular [30]. However, only a single-polarization state can be obtained for the above mentioned CMMs with the same unit-cell structure.

More recently, Ma et al. [32] proposed a double-layer twisted Y shape structure that achieves obvious CD effect and giant optical rotation at different frequencies simultaneously. However, only one kind of circularly polarized waves can be transformed by such CMM with the realization of 90° linear polarization rotation. In this work, we designed a simple asymmetric CMM using bi-layer twisted split-ring structure. The experimental results are in good agreement with the numerical simulation. When a y-polarized EM wave is incident on the proposed sample propagating along backward $(-z)$ direction, it is found that nearly pure left and right circularly and cross-polarized wave with AT effect can be obtained in transmission simultaneously at different resonance frequencies. Induced surface current and electrical field distributions are investigated to clarify the mechanism of the polarization transformation. The proposed CMM has simple geometry but more functionality in different operating frequency bands than the previous designs [12–32], and can be used in applications such as antenna radome, remote sensors and radiometer, polarization spectral filter [40–42].

2. PHYSICAL MODEL, SIMULATION AND EXPERIMENT

Figures 1(a) and (b) show the photograph of a portion of a fabricated CMM sample and schematics of unit-cell structure, which consists of double-layered copper structure patterned on opposite sides of an FR-4 board. With the purpose of giant chirality and AT effect, the mirror symmetry breaking along the propagation direction is the unique route, which enables the lack of structural mirror symmetry [27]. The single-layer planar structure design proposed here is similar to those in [43, 44]; however, it is distinguished in that double split and bi-layer asymmetry are introduced to tailor the cross-coupling
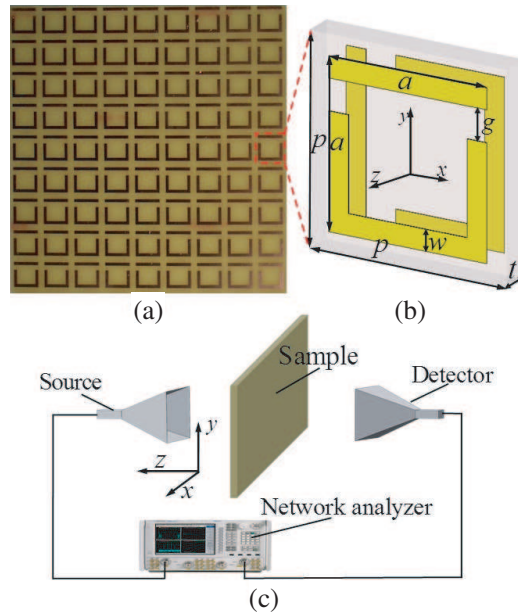

Figure 1. (a) Photograph of a portion of the fabricated sample, (b) perspective view of the unit cell structure, (c) schematic of the transmission coefficients measurement.

between electric and magnetic fields, which can modify the transmission for the y-polarization normal incident wave. As shown in Figure 1(b), for the unit cell structure, the front SRR is rotated 90° with respect to the back one. This unit cell can be repeated to create a layer that can function as a polarizer. Moreover, for a perfect or nearly diodelike AT effect of linearly polarized waves, the one transmission of the two off-diagonal (cross-polarized) components of the Jones matrix (t_{xy} or t_{yx}) should be enhanced, and all the others (t_{yx} or t_{xy}, t_{xx}, t_{yy}) should be suppressed significantly. As a result, diodelike transmission with strong asymmetry takes place for the incident waves which are linearly polarized in the x or y directions [19].

We will demonstrate numerically and experimentally our proposed CMMs for the dual-band circular polarizer and linear polarization transformation with strong AT effect. For the proposed asymmetric CMMs as shown in Figures 1(a) and (b), the relative dielectric constant of the FR-4 board is 4.2 with a dielectric loss tangent of 0.015, and the metallic structure layers in both sides were modeled as a 0.035 mm copper film with an electric conductivity $\sigma = 5.8 \times 10^7$ S/m. The optimal geometry parameters are as follow: $p = 10$ mm, $a = 8$ mm, $w = 1$ mm, $g = 1.5$ mm, $t = 1.5$ mm. The numerical simulations were performed based on the standard finite difference time domain (FDTD) method by using the frequency domain solver of the CST Microwave Studio. In the process of simulation, the periodic boundary conditions were applied to the x and y directions, while perfectly matched layers were applied to the z direction.

For experiments, the designed structures are fabricated into a 20×20 unit cell sample (10 mm $\times$ 10 mm $\times$ 1.57 mm) by the conventional printed circuit board (PCB) process, and the photograph of a portion of a fabricated CMM sample is shown in Figure 1(a). The sample was measured through free-space EM transmission measurement in a microwave anechoic chamber. Agilent PNA-X N5244A vector network analyzer connected to the two standard gain broadband linearly polarized horn antennae was employed to measure the CMM sample in an EM anechoic chamber. The schematic of the transmission coefficients measurement is shown in Figure 1(c). Both antennas own VSWR < 2, and they face each other with a distance of 1 m over a wide frequency range of 4 to 16 GHz to eliminate the near-field effect. In the measurements, the time-domain gating strategy was used to eliminate the undesirable repetitively reflected EM waves [27]. A linearly polarized EM wave ($\boldsymbol{E}$ field in the x or y) direction is incident on the CMM structure sample propagating along $-z(+z)$ direction. Four different linear transmission coefficients could be obtained by rotating the received antennae. Then the linear-to-circular and circular-to-circular transmission coefficients can be calculated from the transformation equations described in [25, 27, 28] in detail.

3. RESULTS AND DISCUSSION

Figures 2(a) and (b) show the simulated and measured linear transmission coefficients and phase difference φ_y between co- and cross-polarizations for the backward propagation in y polarization. A good agreement between simulation and measurement can be observed across the entire frequency range. The electric response for the normally incident x-polarized wave distinguishes from that for the y-polarized wave due to the structure's lack of C4 symmetry [27]. In this particular design, the giant CD effect and good performances for the circular polarizer are only valid for the $(x)y$ polarization incident field propagating along $+z(-z)$ direction. From Figure 2(a), three simulation (measurement) resonant peaks (dips) are obviously observed around $f_1 = 5.36(5.32)$ GHz, $f_2 = 6.65(6.6)$ GHz and $f_3 = 10.47(10.52)$ GHz from the co- and cross-polarization transmission coefficients t_{yy} and t_{xy}. Note that there are a slight frequency shift between simulation and measurement curves, and the possible reasons for this shift can include: (1) the difference of the EM parameters (e.g., permittivity) of the dielectric substrate, (2) the small differences in substrate and metal thicknesses, and (3) the finite size effects also should be considered. Numerical and experimental results both indicate that the peak values of cross-polarization transmission coefficients t_{xy} reach at least 0.5 for three resonant bands. Thus, the high transformation efficiency can be unambiguously demonstrated. The amplitudes of t_{yy} and t_{xy} are nearly the same, and the ratio ($|t_{xy}|/|t_{yy}|$) nearly achieve unity around resonances (f_1 and f_2), respectively. At the third resonant frequency (f_3), the simulation (measurement) amplitude of co-polarization transmission coefficients t_{yy} decreases to the minimum value of 0.032(0.074), while the t_{xy} is up to the maximum value of 0.878(0.917). In addition, as shown in Figure 2(b), phase difference
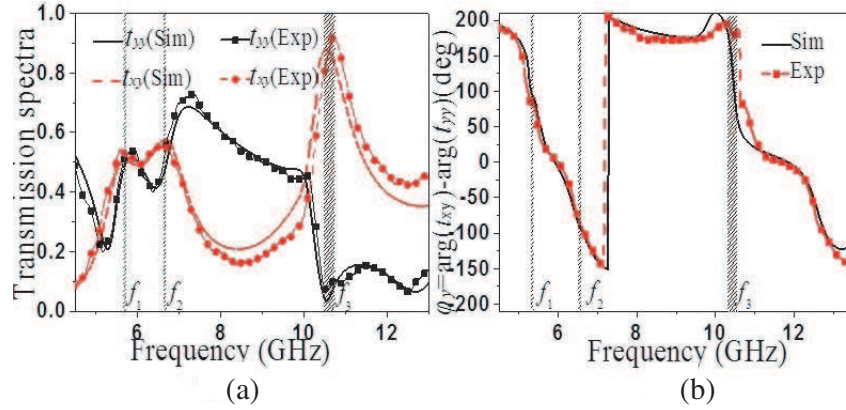
Figure 2. Simulated and measured results for the designed CMM: (a) linear transmission coefficients for the backward propagation in y polarization, (b) phase difference φ_y between t_{xy} and t_{yy}.
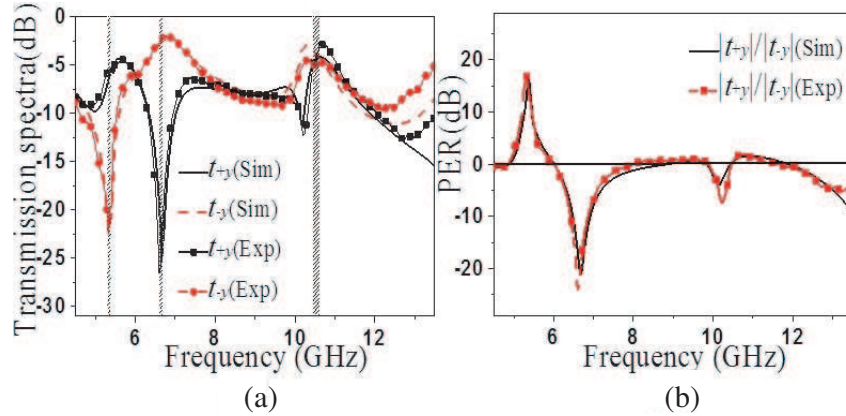

Figure 3. Simulated and measured (a) linear to circular transmission coefficients, (b) polarization extinction ration (PER).

φ_y is about 90°, $-90°$, and 180° around above three resonant frequency points. These results suggest that nearly pure circular polarization waves with different handedness are emitted around two lower resonances (f_1 and f_2), and most of the incident y-polarized wave is transformed into the x-polarized or experienced nearly 90° polarization rotation around higher frequency (f_3) after the y-polarized wave passing through the designed CMMs slab propagating along backward ($-z$) direction. It should be noted that three resonances could also be obtained around the same frequencies for incident x-polarized wave propagation $-z$ direction, but its cross-polarization transmission t_{yx} is much lower than the co-polarization t_{xx} (not shown), thus the transmitted waves are elliptical polarization.

Figures 3(a) and (b) show the numerical and experimental RCP and LCP emitted wave transmission coefficients calculated from the two linear wave transmission coefficients using the transformation equations described in detail in [25]. There are significant differences between the transmission of RCP and LCP waves around the resonances (f_1 and f_2) due to the asymmetric chiral structure along the propagating direction. From Figure 3(a), numerical (experimental) results indicate that the transmitted LCP wave reaches a minimum value of $-23.1(-22.5)$ dB at $5.36(5.32)$ GHz while the RCP wave reaches a minimum value of $-25.3(-26.9)$ dB at $6.65(6.61)$ GHz. At two lower frequencies (f_1 and f_2), it can also be seen that the transmission coefficients of the RCP and LCP wave are $-5.8(-5.6)$ dB and $-2.5(-2.5)$ dB, respectively. As shown in Figure 3(b), the large polarization extinction ratios (PER) of $16.1(16.8)$ dB and $-21.1(-23.8)$ dB can be observed, which indicates the pronounced CD effect at the above two frequencies. It means that the incident y-polarized (x-polarized) along the $-z(+z)$ directions wave can be converted well to the transmitted nearly pure RCP and LCP waves around the resonances
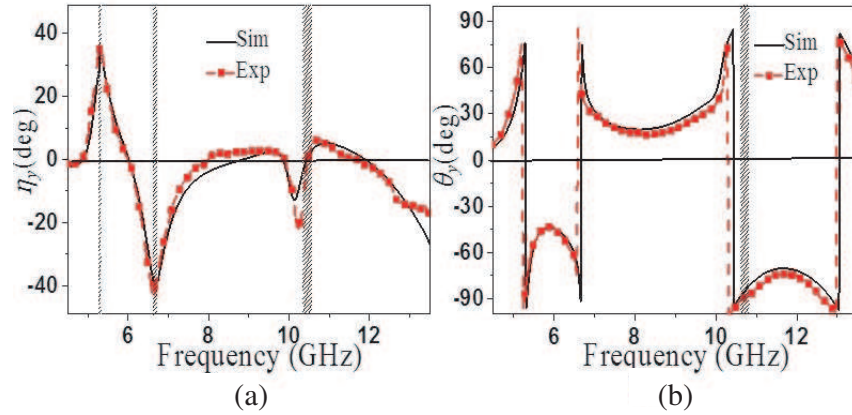
Figure 4. Simulated and measured (a) ellipticity (η) and (b) polarization azimuth rotation angle (θ) for the backward ($-z$) propagation in y polarization.

(f_1 and f_2) after passing through the CMMs slab.

The functionality of dual-band circular polarizer (giant CD effect) and linear polarization transformer (giant optical rotation) of the proposed asymmetric CMMs can be clearly demonstrated through the analysis of ellipticity (η) and the polarization rotation angle (θ) described in detail in [3, 25]. Figures 4(a) and (b) display the ellipticity (η) and polarization azimuth rotation angle (θ) for the y polarization incidence propagating along backward ($-z$) direction. From Figure 4(a), one can see that the simulation (experiment) peak value of η_y is about $35.1°(36.2°)$ and $-41.9°(-44.2°)$ at lower frequency resonances (f_1 and f_2), respectively, for the y-polarized incident wave, further confirming a near pure RCP wave and LCP wave emissions. Moreover, the polarization azimuth rotation angles can be observed as $\theta_y = -43.7°(-43.4°)$ and $-93.2°(-93.7°)$ with respect to the incident linearly y-polarized wave when $\eta_y = 0°$ at $6.0\,\text{GHz}$ and $f_3 = 10.47(10.52)\,\text{GHz}$, revealing a huge optical activity. It can be imagined that the major polarization axis of the emitted wave for y polarization incidence undergoes clockwise rotation rapidly toward x axis ($-90°$), then reaches a negative maximum value of $-93.2°(-93.7°)$ at $10.47(10.52)\,\text{GHz}$, and finally rotates counterclockwise rapidly back to y axis, which is similar to the results of [18, 20, 27]. These results confirm that nearly pure circularly polarized waves with different handedness and near $90°$ rotation linearly polarized wave are realized at two lower frequencies (f_1 and f_2) and higher frequency (f_3) for the designed CMM slab, respectively. Thus, this CMMs slab can be functioned as a simultaneous circular and linear polarizer at different resonances.

In recent years, the AT effect for linear polarization is unusual and appealing polarization functionalities studied due to their potential application, such as optical isolator and circulators [16–21]. According to above results, we can conjecture that the designed structure also function as AT effect for linear polarization only around the third resonance (f_3). In the next section, we will focus on AT effect of the third resonance of the designed structure. To validate this point, the AT parameters for linear and circular polarization bases were calculated [20, 21], and the corresponding results are depicted in Figures 5(a) and (b). It can be clearly seen that the parameter $\Delta_{lin}^{y(x)}$ for linear polarization reaches a positive maximum value of $0.742(0.807)$ while it has a negative minimum value of $-0.742(-0.807)$ at the third frequency of $10.47(10.52)\,\text{GHz}$, which is very comparable with previous results [16, 18, 20, 21]. However, due to the specific asymmetry in the structure, there is almost zero asymmetric transmission for either the RCP or LCP waves across the whole frequency range.

Due to the large AT parameter for the linear polarization of the proposed structure, the total transmission of each linearly polarized wave for both x- and y-polarized incidence waves is quite different along opposite directions [18, 27]. To verify this point, total transmission T_x of emitted x-polarized wave for both x- and y-polarized incidences along the forward ($+z$) and backward ($-z$) directions through the structure are shown in Figure 6(a), where the simulation is in reasonable agreement with measurement. It can be observed that the backward total transmission T_x reaches peak values of $0.773(0.851)$ at $10.51(10.68)\,\text{GHz}$ while the forward total transmission approaches a minimum values of $0.018(0.023)$ at $10.65(10.72)\,\text{GHz}$. Thus, the substantially different total transmissions along the
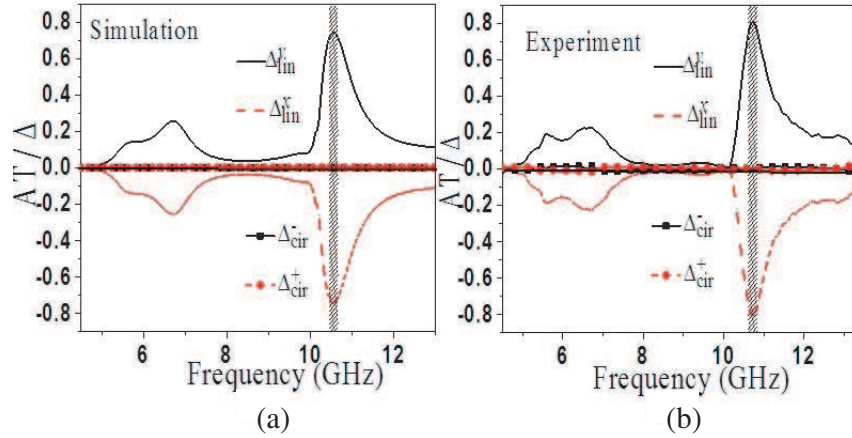
Figure 5. (a) Simulated and (b) measured AT parameter Δ for linear and circular polarization bases.
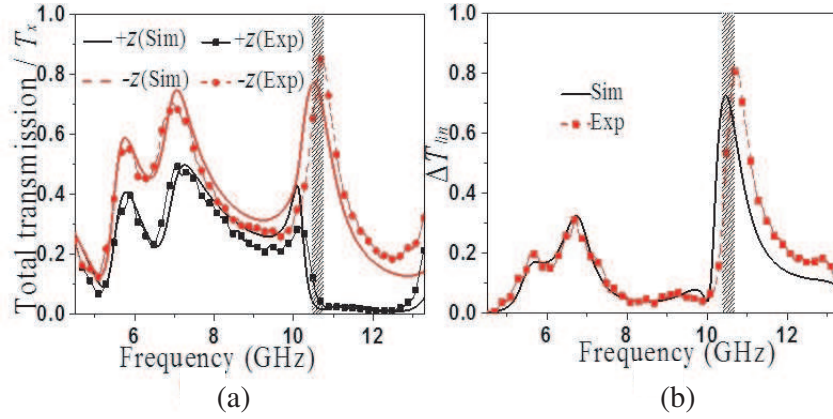

Figure 6. Simulated and experimental results of (a) total transmission of emitted x-polarized wave for both x-polarized and y-polarized incidence along the forward $(+z)$ and backward $(-z)$ directions through the structure, and (b) asymmetry factor (ΔT_{lin}).

two opposite directions indicate a strong asymmetric factor ΔT_{lin} of linear polarization transmission wave, as shown in Figure 6(b). It can also be seen that the asymmetric factor ΔT_{lin} reaches peak values of $0.724(0.814)$ at $10.68(10.72)$ GHz, which reveals a nearly diodelike AT effect. However, for the achievement of perfect diodelike AT effect, the $t_{xx} \approx 0$, $t_{yx} \approx 0$, $t_{yy} \approx 0$, and $t_{xy} \approx 1$ must be achieved for backward propagation, which will lead to $\Delta T_{lin} \approx 1$. Note that the asymmetry factor is strongly dependent on the incident polarization and has its maximum for the x- and y-polarized waves [19].

Intrinsically, the giant CD effect and asymmetric optical activity for different polarizations mainly originate from the interlayer near-field coupling between two twisted layers [35, 36]. Thus, the resonant polarization conversion can be tailored by the EM coupling. Around these resonant frequencies, all the field patterns will be twisted inside the slab as a consequence of interlayer coupling [20, 21]. Surface current distributions are studied in the unit-cell of CMMs to observe the coupling between the electric and magnetic fields, as shown in Figures 7(a), (b) and (c). From Figures 7(a) and (b), similar to the results of [15, 28], the currents on the front and back SRRs are in the same direction at the first frequency (5.36 GHz), and the antiparallel current exists on the top and bottom layers of the structure at the second frequency (6.65 GHz), which are symmetric resonance mode as coupled electric dipoles resonance and asymmetric resonance mode as coupled magnetic dipoles, respectively. Thus, the fundamental electric resonance mode of the first SRR can be excited efficiently, and the near-field coupling between the first and second SRRs results in a emitted RCP and LCP wave at resonances, respectively. From Figure 7(c), at 10.47 GHz, the case is complex and complete, and stronger antiparallel current only exists on the

up, down and left branches of the chiral structure, which will cause the induced magnetic fields mainly parallel to y-direction. Then the electric field along x-direction would be excited by the magnetic field, resulting in the cross-polarization transmission for the y-polarized incident wave propagating along $-z$ direction.

Taking a further step, the evolution of electric fields in the y-z plane of the middle of unit-cell structure including incoming regime, substrate and the outgoing regime is also investigated to provide a direct, intuitionistic witness and understanding of the resonant polarization conversion, as shown in Figures 7(d), (e) and (f). From Figures 7(d) and (e), at 5.36 GHz and 6.65 GHz, after the same y-polarized incident wave passing through the structure propagating along $-z$ direction, the electric fields of outgoing wave will twist to right and left directions, respectively. As shown in Figure 7(f), at 10.47 GHz, it can be seen clearly that the electric field of outgoing wave is along $-x$ direction. It can also be conjectured that the 90% of field strength of incoming wave with y-polarization is transformed to the outgoing wave with x-polarization, coinciding well with the observed cross-coupled transmitted coefficients. These electric field evolution pictures are excellently consistent with the calculated results of the polarization azimuth rotation angle and ellipticity.
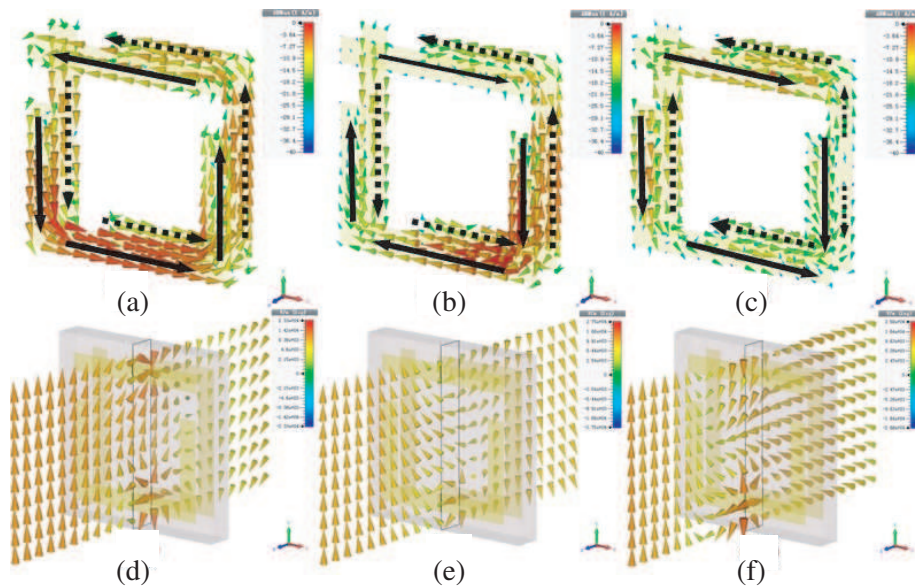

Figure 7. The simulation results of the surface currents distributions and electric fields for the proposed CMMs in the case of y-polarized incident wave propagating along $-z$ direction: (a) and (d) RCP wave at $f_1 = 5.36$ GHz, (b) and (e) LCP wave at $f_2 = 6.65$ GHz, (c) and (f) 90° linear polarization rotation wave at $f_3 = 10.47$ GHz. The solid (dashed) line arrows represent the front (back) surface current direction.

4. CONCLUSION

In summary, an asymmetric CMMs composed of bi-layer twisted SRR structure was proposed and comprehensively characterized by simulation and experiment. The numerical simulation is in good agreement with the measured results, which reveals that the giant CD effect for circular polarized wave emissions with dual bands and linear polarization transformation with near diodelike AT effect can be obtained simultaneously from linearly polarized incident wave at microwave frequencies. The interlayer near-field coupling between two twisted layers of this design has been further illustrated by simulated surface current distributions and electric fields. In addition, if the dimensions are reduced to micro-, nano- and even lower scale, the operation frequency of the proposed CMM can also be scaled to other EM spectrums, such as millimeter wave, terahertz, or even optical range. The proposed CMM structure could also be beneficial in designing optical functional materials, such as polarization spectral filter, circular polarizer, optical isolator and circulators.

ACKNOWLEDGMENT

REFERENCES

1. Tretyakov, S., I. Nefedov, A. Sihvola, S. Maslovski, and C. Simovski, "Waves and energy inchiral nihility," *Journal of Electromagnetic Waves and Applications*, Vol. 17, No. 5, 695–706, 2003.

2. Pendry, J. B., "A chiral route to negative refraction," *Science*, Vol. 306, No. 19, 1353–1355, 2004.

3. Jackson, J. D., *Classical E Lectrodynamics*, 3rd Edition, 205–207, Wiley, 1999.

4. Rogacheva, A. V., V. A. Fedotov, A. S. Schwanecke, and N. I. Zheludev, "Giant gyrotropy due to electromagnetic-field coupling in a bilayered chiral structure," *Phys. Rev. Lett.,* Vol. 97, No. 17, 177401, 2006.

5. Plum, E., J. Zhou, J. Dong, V. A. Fedotov, T. Koschny, C. M. Soukoulis, and N. I. Zheludev, "Metamaterial with negative index due to chirality," *Phys. Rev. B*, Vol. 79, No. 3, 035407(6), 2009.

6. Zhou, J., J. Dong, B. Wang, T. Koschny, M. Kafesaki, and C. M. Soukoulis, "Negative refractive index due to chirality," *Phys. Rev. B,* Vol. 79, No. 12, 121104(4), 2009.

7. Li, Z., R. Zhao, T. Koschny, M. Kafesaki, K. B. Alici, E. Colak, H. Caglayan, E. Ozbay, and C. M. Soukoulis, "Chiral metamaterials with negative refractive index based on four "U" split ring resonators," *Appl. Phys. Lett.,* Vol. 97, No. 8, 081901(3), 2010.

8. Dincer, F., C. Sabah, M. Karaaslan, E. Unal, M. Bakir, and U. Erdiven, "Asymmetric transmission of linearly polarized waves and dynamically wave rotation using chiral metamaterial," *Progress In Electromagnetics Research*, Vol. 140, 227–239, 2013.

9. Li, J., F.-Q. Yang, and J.-F. Dong, "Design and simulation of L-shaped chiral negative refractive index structure," *Progress In Electromagnetics Research*, Vol. 116, 395–408, 2011.

10. Song, K., X.-P. Zhao, Q. H. Fu, Y. H. Liu, and W. R. Zhu, "Wide-angle 90°-polarization rotator using chiral metamaterial with negative refractive index," *Journal of Electromagnetic Waves and Applications,* Vol. 26, Nos. 14–15, 1967–1976, 2012.

11. Cheng, Y., Y. Nie, and R. Z. Gong, "Giant optical activity and negative refractive index using complementary U-shaped structure assembly," *Progress In Electromagnetics Research M,* Vol. 25, 239–253, 2012.

12. Decker, M., M. W. Klein, M. Wegener, and S. Linden, "Circular dichroism of planar chiral magnetic metamaterials," *Opt. Lett.*, Vol. 32, No. 7, 856–858, 2007.

13. Gansel, J., M. Thiel, M. S. Rill, M. Decker, K. Bade, V. Saile, G. von Freymann, S. Linden, and M. Wegener, "Gold helix photonic metamaterial as broadband circular polarizer," *Science*, Vol. 325, No. 5947, 1513–1515, 2009.

14. Zhao, Y., M. A. Belkin, and A. Alù, "Twisted optical metamaterials for planarized ultrathin broadband circular polarizers," *Nat. Commun.*, Vol. 3, 870, 2012.

15. Cheng, Y., Y. Nie, L. Wu, and R. Z. Gong, "Giant circular dichroism and negative refractive index of chiral metamaterial based on split-ring resonators," *Progress In Electromagnetics Research*, Vol. 138, 421–432, 2013.

16. Menzel, C., C. Helgert, C. Rockstuhl, E.-B. Kley, A. Täunnermann, T. Pertsch, and F. Lederer, "Asymmetric transmission of linearly polarized light at optical metamaterials," *Phys. Rev. Lett.*, Vol. 104, 253902, 2010.

17. Wei, Z. Y. Cao, Y. Fan, X. Yu, and H. Li, "Broadband polarization transformation via enhanced asymmetric transmission through arrays of twisted complementary split-ring resonators," *Appl. Phys. Lett.*, Vol. 99, No. 22, 221907-3, 2011.

18. Huang, C., Y. Feng, J. Zhao, Z. Wang, and T. Jiang, "Asymmetric electromagnetic wave transmission of linear polarization via polarization conversion through chiral metamaterial structures," *Phys. Rev. B*, Vol. 85, 195131, 2012.

19. Mutlu, M., A. E. Akosman, A. E. Serebryannikov, and E. Ozbay, "Diodelike asymmetric transmission of linearly polarized waves using magnetoelectric coupling and electromagnetic wave tunneling," *Phys. Rev. Lett.*, Vol. 108, 213905, 2012.

20. Cheng, Y. Z., Y. Nie, X. Wang, and R. Z. Gong, "An ultrathin transparent metamaterial polarization transformer based on a twist-split-ring resonator," *Appl. Phys., A Mater. Sci. Process.*, Vol. 111, No. 1, 209–215, 2013.

21. Cheng, Y., Y. Nie, Z. Z. Cheng, L. Wu, X. Wang, and R. Z. Gong, "Broadband transparent metamaterial linear polarization transformer based on triple-split-ring resonators," *Journal of Electromagnetic Waves and Applications*, Vol. 27, No. 14, 1850–1858, 2013.

22. Mutlu, M., A. E. Akosman, A. E. Serebryannikov, and E. Ozbay, "Asymmetric chiral metamaterial circular polarizer based on four U-shaped split ring resonators," *Opt. Lett.*, Vol. 36, No. 9, 1653–1655, 2011.

23. Ye, Y., X. Li, F. Zhuang, and S. W. Chang, "Homogeneous circular polarizers using a bilayered chiral metamaterial," *Appl. Phys. Lett.*, Vol. 99, 031111, 2011.

24. Ma, X., C. Huang, M. Pu, C. Hu, Q. Feng, and X. Luo, "Multi-band circular polarizer using planar spiral metamaterial structure," *Opt. Express*, Vol. 20, No. 14, 16050–16058, 2012.

25. Yana, S. and G. A. E. Vandenbosch, "Compact circular polarizer based on chiral twisted double split-ring resonator," *Appl. Phys. Lett.*, Vol. 102, 103503, 2013.

26. Xie, L., H.-L. Yang, X. Huang, and Z. Li, "Multi-band circular polarizer using archimedean spiral structure chiral metamaterial with zero and negative refractive index," *Progress In Electromagnetics Research*, Vol. 141, 645–657, 2013.

27. Xu, H.-X., G.-M. Wang, M.-Q. Qi, and T. Cai, "Dual-band circular polarizer and asymmetric spectrum filter using ultrathin compact chiral metamaterial," *Progress In Electromagnetics Research*, Vol. 143, 243–261, 2013.

28. Cheng, Y. Z., Y. Nie, C. Z. Cheng, X. Wang, and R. Z. Gong, "Asymmetric chiral metamaterial circular polarizer based on twisted split-ring resonator," *Appl. Phys. B*, 2013, DOI 10.1007/s00340-013-5659-z.

29. Wu, L., Z. Y. Yang, Y. Z. Cheng, Z. Q. Lu, P. Zhang, M. Zhao, R. Z. Gong, X. H. Yuan, Y. Zheng, and J. A. Duan, "Electromagnetic manifestation of chirality in layer-by-layer chiral metamaterials," *Opt. Express*, Vol. 21, 5239–5246, 2013.

30. Wu, L., Z. Y. Yang, Y. Z. Cheng, M. Zhao, R. Z. Gong, Y. Zheng, J. A. Duan, and X. H. Yuan, "Giant asymmetric transmission of circular polarization in layer-by-layer chiral metamaterials," *Appl. Phys. Lett.*, Vol. 103, 021903, 2013.

31. Wu, C., H. Li, X. Yu, F. Li, H. Chen, and C. T. Chan, "Metallic helix array as a broadband wave plate," *Phys. Rev. Lett.*, Vol. 107, No. 17, 177401, 2011.

32. Ma, X., C. Huang, M. Pu, W. Pan, Y. Wang, and X. Luo, "Circular dichroism and optical rotation in twisted Y-shaped chiral metamaterial," *Appl. Phys. Exp.*, Vol. 6, 022001, 2013.

33. Zhao, R., J. Zhou, T. Koschny, E. N. Economou, and C. M. Soukoulis, "Repulsive casimir force in chiral metamaterials," *Phys. Rev. Lett.*, Vol. 103, No. 10, 103602, 2009.

34. Zhao, R., T. Koschny, E. N. Economou, and C. M. Soukoulis, "Repulsive Casimir forces with finite-thickness slabs," *Phys. Rev. B*, Vol. 83, No. 7, 075108, 2011.

35. Liu, H., Y. M. Liu, T. Li, S. M. Wang, S. N. Zhu, and X. Zhang, "Coupled magnetic plasmons in metamaterials," *Phys. Status Solidi B*, Vol. 246, 1397, 2009.

36. Liu, N., H. Liu, S. Zhu, and H. Giessen, "Stereometamaterials," *Nat. Photon.*, Vol. 3, 157, 2009.

37. Born, M. and E. Wolf, *Principles of Optics*, Cambridge University Press, 1999.

38. Chen, C. Y., T. R. Tsai, C. L. Pan, and R. P. Pan, "Room temperature terahertz phase shifter based on magnetically controlled birefringence in liquid crystals," *Appl. Phys. Lett.*, Vol. 83, 4497, 2003.

39. Yamada, I., K. Takano, M. Hangyo, M. Saito, and W. Watanabe, "Terahertz wire-grid polarizers with micrometer-pitch Al gratings," *Opt. Lett.*, Vol 34, 274, 2009.

40. Euler, M., V. Fusco, R. Cahill, and R. Dickie, "325 GHz single layer sub-millimeter wave FSS based split slot ring linear to circular polarization convertor," *IEEE Trans. Antenn. Propag.*, Vol. 58, No. 7, 2457–2459, 2010.

41. Zari, D., H. Oraizi, and M. Soleimani, "Improved performance of circularly polarized antenna using semi-planar chiral metamaterial covers," *Progress In Electromagnetics Research*, Vol. 123, 337–354, 2012.

42. Shi, J. H., H. F. Ma, W. X. Jiang, and T. J. Cui, "Multiband stereometamaterial-based polarization spectral filter," *Phys. Rev. B*, Vol. 86, 035103, 2012.

43. Plum, E., X. X. Liu, V. A. Fedotov, Y. Chen, D. P. Tsai, and N. I. Zheludev, "Metamaterials: Optical Activity without Chirality," *Phys. Rev. Lett.*, Vol. 102, No. 11, 113902-4, 2009.

44. Feng, C., Z. B. Wang, S. Lee, J. Jiao, and L. Li, "Giant circular dichroism in extrinsic chiral metamaterials excited by off-normal incident laser beams," *Opt. Communications,* Vol. 285, 2750–2754, 2012.